Mutations of *CD40* gene cause an autosomal recessive form of immunodeficiency with hyper IgM

Simona Ferrari*†, Silvia Giliani*†, Antonella Insalaco*, Abdulaziz Al-Ghonaium‡, Anna R. Soresina*, Michael Loubser‡, Maria A. Avanzini§, Massimo Marconi§, Raffaele Badolato*, Alberto G. Ugazio*¶, Yves Levy‖, Nadia Catalan, Anne Durandy**, Abdelghani Tbakhi‡, Luigi D. Notarangelo*, and Alessandro Plebani*††**

*Istituto di Medicina Molecolare ''Angelo Nocivelli,'' Clinica Pediatrica, Università di Brescia, Piazzale Spedali Civili 1, 25123 Brescia, Italy; ‡King Faisal Specialist Hospital and Research Centre, Riyadh, Saudi Arabia 11211; §Istituto di Clinica Pediatrica, Università di Pavia, 27100 Pavia, Italy; ‖Institut National de la Santé et de la Recherche Médicale, Hôpital Henri Mondor, 94010 Creteil, France; and **Institut National de la Santé et de la Recherche Médicale U429, Hôpital Necker-Enfantes Malades, 75015 Paris, France

Communicated by Max D. Cooper, University of Alabama, Birmingham, AL, August 29, 2001 (received for review April 20, 2001)

CD40 is a member of the tumor necrosis factor receptor superfamily, expressed on a wide range of cell types including B cells, macrophages, and dendritic cells. CD40 is the receptor for CD40 ligand (CD40L), a molecule predominantly expressed by activated CD4$^+$ T cells. CD40/CD40L interaction induces the formation of memory B lymphocytes and promotes Ig isotype switching, as demonstrated in mice knocked-out for either *CD40L* or *CD40* gene, and in patients with X-linked hyper IgM syndrome, a disease caused by *CD40L*/*TNFSF5* gene mutations. In the present study, we have identified three patients with an autosomal recessive form of hyper IgM who fail to express CD40 on the cell surface. Sequence analysis of *CD40* genomic DNA showed that one patient carried a homozygous silent mutation at the fifth base pair position of exon 5, involving an exonic splicing enhancer and leading to exon skipping and premature termination; the other two patients showed a homozygous point mutation in exon 3, resulting in a cysteine to arginine substitution. These findings show that mutations of the *CD40* gene cause an autosomal recessive form of hyper IgM, which is immunologically and clinically undistinguishable from the X-linked form.

Cognate signaling between helper T cells and B cells involves a series of interactions between receptors and counterreceptors. Activated CD4$^+$ T cells express CD40 ligand (CD40L), which engages CD40 on resting B cells and accounts for most cell contact-dependent T cell help for B cells (1, 2). CD40 activation is critical for B cell proliferation, Ig isotype switching, and germinal center formation (3). The critical role of CD40/CD40L interaction is underscored by the defects observed in patients with X-linked hyper IgM syndrome (HIGM1), who have a defect of CD40L expression because of mutations in the *TNFSF5* gene (4–7). Because of defective T helper activity, B lymphocytes from HIGM1 patients express only surface IgM and IgD, and the antibody response is restricted to the IgM isotype (8). In accordance with this concept, B lymphocytes obtained from HIGM1 patients proliferate and produce normal amounts of immunoglobulins (including IgM, IgG, IgA, and IgE) if appropriately stimulated *in vitro* with anti-CD40 and lymphokines (9, 10), suggesting that HIGM1 is a primary T cell disorder. Similarly, CD40L-deficient mice show defective antibody formation and lack of Ig switching, and their lymphoid tissue is devoid of germinal centers (11). A similar phenotype has been observed in CD40-deficient mice as well (12, 13); however, genetic defects of CD40 have not been reported in humans so far.

Although the hyper IgM syndrome is most commonly inherited as an X-linked trait (HIGM1), reports of autosomal recessive and autosomal dominant forms of the disease have indicated the existence of other genetic defects (8). These forms of hyper IgM syndrome are characterized by lack of *TNFSF5* gene mutations and by normal membrane expression of CD40L (CD40L$^+$ HIGM). B cells from these patients do not undergo class switch recombination *in vitro* in the presence of CD40-agonists, suggesting that the defect(s) of CD40L$^+$ forms of hyper IgM is (are) intrinsic to B cells (14, 15). Recently, it has been shown that mutations of the activation-induced cytidine deaminase (*AID*) gene are responsible for HIGM2, one of the autosomal recessive forms of hyper IgM syndrome (16).

However, mutations of the *AID* gene do not account for all cases of autosomal recessive HIGM syndrome in humans, suggesting that other genes may be involved. In this study, we demonstrate that two independent mutations of the *CD40* gene, leading to lack of surface expression of CD40, cause an autosomal recessive form of immunodeficiency with hyper IgM (HIGM3), which is characterized by lack of Ig isotype switching, impaired generation of memory B cells, and defective somatic hypermutation.

Materials and Methods

Flow Cytometry. Peripheral blood mononuclear cells (PBMC) were isolated by Ficoll-Hypaque density centrifugation. Immunofluorescent studies were performed by using the following antibodies: FITC-labeled anti-human CD40 (5C3 mAb), FITC-labeled anti-human IgD (IA6-2 mAb), phycoerythrin (PE)-labeled anti-human IgM (G20-127 mAb), and PE-labeled anti-human CD19 (HIB19 mAb) from PharMingen; PE-labeled anti-human CD27 (L128 mAb) and PerCP-labeled anti-human CD20 (L27 mAb) from Becton Dickinson. PBMC were resuspended in PBS/0.1% BSA (PBS/BSA) at the concentration of 5×10^5–5×10^6 cells/ml and incubated at 4°C for 30 min with 5 μl of the properly commercial antibodies. After staining, the cells were washed twice with PBS/BSA and fixed in 2% paraformaldehyde in PBS. Samples were then analyzed by FACSCalibur (Becton Dickinson).

Western Blot. Epstein–Barr virus (EBV)-transformed B cell lines (B-LCL, 2×10^6) were lysed with 30 μl lysis buffer (300 mM NaCl/50 mM Tris·Cl, pH 7.5/2 mM EDTA/0.5% Triton X-100/protease inhibitors) for 15 min on ice and centrifuged for 10 min at 14,000 $\times$ *g*. SDS gel-loading buffer was added to the super-

Abbreviations: HIGM, human hyper IgM immunodeficiency; B-LCL, Epstein–Barr virus-transformed lymphoblastoid B cell line; PBMC, peripheral blood mononuclear cells; STAT, signal transducers and activators of transcription; Pt., patient; CD40L, CD40 ligand; PE, phycoerythrin; RT-PCR, reverse transcription–PCR.

†S.F. and S.G. contributed equally to this work

¶Present address: Ospedale Pediatrico Bambino Gesú, Roma, Italy.

††To whom reprint requests should be addressed. E-mail: plebani@master.cci.unibs.it.

The publication costs of this article were defrayed in part by page charge payment. This article must therefore be hereby marked "*advertisement*" in accordance with 18 U.S.C. §1734 solely to indicate this fact.

 www.pnas.org/cgi/doi/10.1073/pnas.221456898

natant, and the samples were boiled for 3 min. The proteins were separated by 10% SDS-polyacrylamide gel, transferred to poly(vinylidene difluoride) (PVDF) membrane (Immobilon-P-Millipore) and probed with an affinity-purified rabbit polyclonal antibody raised against the amino terminus of CD40 (sc-974-Santa Cruz). The blot was developed by the enhanced chemiluminescence (ECL) Western blotting detection system (Amersham Pharmacia). The filter was stripped and reprobed with an affinity-purified rabbit polyclonal antibody raised against the carboxyl terminus of CD40 (sc-975-Santa Cruz) or with an anti-STAT5 (signal transducers and activators of transcription 5) antibody as control.

Human *CD40* Gene Analysis. The human *CD40* gene structure was determined by alignment of the CD40 mRNA sequence (accession no. NM 001250) with a contig derived from assembled genomic sequence data (accession no. AL035662.60). The nine exons of human *CD40* gene were amplified by PCR with the following primers. Primers for exon 1: 5′-ATAGGTGGAC-CGCGATTGGT-3′ (forw); 5′-TCCCAACTCCCGTCT-GGT-3′ (rev). Primers for exon 2: 5′-GCTGAAGAAGTTG-CAACGGA-3′ (forw); 5′-AAAGCAAAGGGGGACTCCA-3′ (rev). Primers for exon 3: 5′-GTTAGTGTCTGACTCAT-GGA-3′ (forw); 5′-AATGGCTGCATTGTCGGGA-3′ (rev). Primers for exon 4: 5′-GGTCTGAGGAAGAAAGAGCA-3′ (forw); 5′-CTTGGGCCCTAAGCTCCT-3′ (rev). Primers for exon 5: 5′-GTGGTCCACTGTGATGGTTA-3′ (forw); 5′-GAGGCCACTCTGCAGATGCT-3′ (rev). Primers for exon 6: 5′-GTTGTGTGCTCAGTGAACCT-3′ (forw); 5′-ACCTTC-CTAGGCTTTCTCCA-3′ (rev). Primers for exon 7: 5′-GTAGGGAGAAACTGCAGGT-3′ (forw); 5′-CCAGATAA-GAAACAGGTGGT-3′ (rev). Primers for exon 8: 5′-GTAGGGAGAAACTGCAGGT-3′ (forw); 5′-GTTTTACT-GCCCCATAGGCA-3′ (rev). Primers for exon 9: 5′-AGGGGCTCCTCAGAGGCA-3′ (forw); 5′-CTCTCTGGC-CAACTGCCT-3′ (rev). For exons 1, 2, 4, 5, and 9, PCR was performed with 2.5 units of *Taq* Gold polymerase (Perkin–Elmer): 1 cycle at 95°C for 10 min, and 35 cycles at 94°C for 30 s, at 65°C for 30 s, and at 72°C 30 s. For exons 3, 6, 7, and 8, PCR was performed with 1 unit of *Taq* polymerase (Perkin–Elmer): 1 cycle at 94°C for 5 min, and 35 cycles at 94°C for 30 s, at 58°C for 30 s, and at 72°C for 30 s. PCR products were purified by using Microcon centrifuge filters (Amicon-Millipore), sequenced with dRhodamine dye terminator cycle sequencing kit (PE-Applied Biosystems), and analyzed with the Applied Biosystems Prism 310 genetic analyzer.

Human CD40 Transcripts Analysis. Total RNA from fresh PBMC was extracted by using NucleoSpin RNA II kit (Macherey & Nagel). The reverse transcription reaction was performed starting from 1–3 μg of total RNA and random hexamers (GeneAmp RNA PCR Core kit; Perkin–Elmer).

Reverse transcription (RT)-PCR was performed with the following primers: P1, 5′-GGTTCGTCTGCTCTGCAGT-3′; P2, 5′-CAACATCAGTCTTGTTTGTGCCT-3′; P3, 5′-CCT-GTGAGAGCTGTGTCCT-3′; P4, 5′-GGTTGTGCAACAG-GCAGGCA-3′; and P5, 5′-CTCTCTGGCCAACTGCCT-3′. PCR products were cloned in the pCR-2.1 vector by using the TOPO-TA cloning kit (Invitrogen), and positive clones were sequenced as described above. Amplification of β-actin transcripts was performed as an internal control (primers available on request).

Exon Trapping Experiment. The exon trapping experiment, originally developed by Buckler *et al.* (17) and modified by Church *et al.* (18), was performed by using the Exon Trapping System (GIBCO/BRL), according to the protocol recommended by the manufacturer. The method can be divided into three distinct steps: (*i*) subcloning of genomic DNA, containing either wild-type or mutant *CD40* exon 5, into the exon trapping vector pSPL3; (*ii*) transfection of the selected recombinant pSPL3 clones into COS-7 cells; and (*iii*) analysis of the RNA isolated from transiently transfected cells for the presence of trapped *CD40* exon 5 sequence.

Vector construction. The wild-type or mutant PCR products, containing the entire exon 5 (94 bp), flanked by 329 bp corresponding to part of the intron 4 and 140 bp corresponding to part of the intron 5, respectively, were obtained by using the following oligonucleotides: 5′-AGGAGCTTAGGGCCCAAGGT-3′ (forw) and 5′-GAGGCCACTCTGCAGATGCT-3′ (rev), and subcloned in the pCR-2.1 vector by using the TOPO-TA cloning kit (Invitrogen). *Bam*HI-*Eco*RV fragments were generated from this plasmid, gel-purified, and inserted into the pSPL3 vector linearized with the same restriction endonucleases. The pSPL3 derivatives were propagated in *E. coli*, and the DNA was purified and transfected into COS-7 cells.

COS-7 transfection. COS-7 cells were propagated in DMEM supplemented by 10% FBS, glutamine, and nonessential amino acids. For transfection, 4×10^5 cells were seeded in 3.5-cm, six-well dishes, and grown to 70–80% confluence. Transfection was performed by using GIBCO/BRL LIPOFECTACE reagent, as recommended in the standard protocol. Transfected cells were incubated in supplemented DMEM for 24 h at 37°C in a 5% CO_2 incubator, and total RNA was isolated by using NucleoSpin RNA II kit (Macherey & Nagel).

Exon amplification. Total RNA was used for the synthesis of first-strand cDNA, catalyzed by SUPERSCRIPT II RNase H^- Reverse Transcriptase. The cDNA was amplified by PCR using oligonucleotides that were complementary to the splicing vector. In particular, for the primary PCR, oligonucleotides SD6 (5′-TCTGAGTCACCTGGACAACC-3′) and SA2 (5′-ATCT-CAGTGGTATTTGTGAGC-3′) were used, and for the secondary PCR, oligonucleotides dUSD2 (5′-CUACUACUACU-AGTGAACTGCACTGTGACAAGCTGC-3′) and dUSA4 (5′-CUACUACUACUAAGGAGTGAATTGGTCG-3′) were used. The secondary PCR products were electrophoresed through 2% agarose gel and blotted on Hybond-N+ nylon membrane (Amersham Pharmacia). The filter was hybridized to radiolabeled DNA probe corresponding to *CD40* exon 5, by using a standard procedure. The secondary PCR products were cloned in pAMP10 and sequenced by using primer SD2 (5′-GTGAACTGCACTGTGACAAGCTGC-3′).

***In Vitro* Immunoglobulin Production.** PBMC (10^5/well) were cocultured with 2×10^3/well irradiated (70 Gy) CDw32FcγRII-transfected L cells and 0.5 μg/ml anti-CD40 mAb89, in the presence or not of recombinant human IL-10 (200 ng/ml; Genzyme). All cultures were set up in Iscove's medium, supplemented with 50 μg/ml human transferrin, 5 μg/ml bovine insulin, 0.5% BSA, 5×10^{-5} M 2β-mercaptoethanol, and 5% heat-inactivated FBS. All conditions were run in triplicate to a final volume of 200 μl/well. The supernatants were harvested after 10 days of culture at 37°C in humidified 5% CO_2, and Ig production was assessed by an ELISA technique.

Results and Discussion

Immunological Phenotype of HIGM3 Patients. To characterize the molecular basis of immunodeficiency with hyper IgM in patients with normal CD40L expression and lack of mutations in the *AID* gene, we systematically evaluated the expression of B cell differentiation markers in hypogammaglobulinemic patients.

We identified three children: an 8-year-old Italian female [Patient 1 (Pt. 1)] born from consanguineous parents, and two first cousins, a 5-year-old male (Patient 2) and a 7-year-old female (Patient 3) from a multiply related Saudi Arabian family, who all shared normal counts of circulating B cells and a

Table 1. Immunological profile of HIGM3 patients

Patient no.	Immunoglobulin serum level, mg/dl			Lymphocyte subsets, %				Lymphocyte proliferation, cpm $\times 10^{-3}$		
	IgG	IgA	IgM	CD3	CD4	CD8	CD19	Medium	PHA	α-CD3
1	180	<6.67	81	73	55	13	16	1.35	124.2	82.1
2	Und	Und	400	75	35	24	19	1.15	122	ND
3	Und	Und	200	76	54	19	20	0.95	138	ND
Normal range	351–1,916	17–178	48–337	64–78	33–47	20–30	12–24	0.97–1.5	115.6–188.5	71.5–120.8

Und, undetectable; ND, not done.

profound reduction of IgG and IgA serum levels, whereas IgM were present at normal/high levels (Table 1).

Pt.1 was admitted to a local hospital at the age of 4 months for a severe respiratory distress because of *Pneumocystis carini* infection. At the age of 2 years, she was again hospitalized for another episode of pneumonia and was found to have hypogammaglobulinemia with normal levels of IgM. Since then, she has been on Ig substitution therapy.

Pt.2 and Pt.3 suffered from recurrent lower respiratory tract infections from the age of 6 months and 8 months, respectively. For Pt.2, the diagnosis of hypogammaglobulinemia with high levels of IgM and severe neutropenia was made at the age of 16 months, and regular Ig substitution therapy and granulocyte-colony-stimulating factor administration were started. For Pt.3, the diagnosis of hypogammaglobulinemia with normal levels of IgM was made at 8 months, and Ig replacement therapy was initiated. At the age of 3 years, she was admitted to an intensive care unit because of interstitial pneumonia.

The peripheral $CD3^+$ T lymphocyte and B lymphocyte counts were normal for all three patients, and so were *in vitro* lymphocyte proliferative responses to phytohemagglutinin or anti-CD3 (Table 1). Furthermore, normal delayed hypersensitivity to tetanus toxoid was recorded in Pt.1.

Defective Expression of CD40 in HIGM3 Patients. Flow cytometry profiles showed lack of CD40 expression on the surface of peripheral blood B lymphocytes (Fig. 1), monocytes, and B-LCLs derived from Pt.1 and Pt.2 (data not shown). Western-blot analysis of B-LCL lysates, performed by using an anti-CD40 polyclonal antibody directed against the amino terminus of CD40, showed complete lack of CD40 protein in Pt.1, whereas a band with an apparently lower molecular weight was revealed in Pt.2 as compared with normal controls (Fig. 2). As expected, both the normal band and the lower molecular weight band were present in the patient's mother (Pt.2 Mo in Fig. 2). Equal amounts of protein extract were loaded for each sample, as shown by reblotting with an anti-STAT5 antibody. The same results as in Fig. 2 were obtained by using an antibody directed against the carboxyl terminus of the CD40 protein (data not shown).

To investigate the molecular basis of defective CD40 expression, we performed RT-PCR analysis of CD40 mRNA obtained from PBMC or B-LCLs. The CD40 transcript was amplified with exonic primers that span the region from exon 1 to 6 (P1 and P2 in Fig. 3). In Pt.1, the only detected specific product was smaller than the 550-bp-long fragment amplified from normal controls (Fig. 3). As expected, both a normal-sized and the smaller-sized amplification products were simultaneously obtained from the patient's mother (the father could not be investigated because he was not available). In contrast, a normal-sized product was obtained in Pt.2 (Fig. 3). The CD40 amplification products obtained by using primers encompassing exons 6 to 9 (P4 and P5 in Fig. 3) were identical both in patients and in normal individuals (data not shown).

Direct sequence analysis of the mutant cDNA product from Pt.1 showed a deletion of 94 nt (from nucleotide 451 to 544), precisely matching the entire sequence of exon 5. Skipping of exon 5 was confirmed by sequence analysis of 10 independent clones obtained from Pt.1 cDNA.

In agreement with the RT-PCR data, the same deletion was also present in approximately half of the cDNA clones obtained from the patient's mother. Lack of exon 5 causes a frameshift after amino acid 135, leading to premature termination at codon 191, within exon 7. Presumably, the truncated protein is unstable and rapidly degraded, as indicated by lack of protein detection by Western-blot analysis (Fig. 2).

Because it is known that several isoforms of CD40 mRNA are normally generated by exon skipping (19), the possibility that the deleted PCR product found in Pt.1 represented a normal alternative transcript had to be ruled out. cDNA clones spanning the entire CD40 transcript were generated from LCL from two independent normal individuals, by using primers P1 and P2 (Fig. 3, exons 1–6), and P3 and P5 (Fig. 3, exons 4–9). After analysis of over 50 clones, skipping of exon 5 was never observed; on the other hand, about 15% of the clones lacked exon 6 or exon

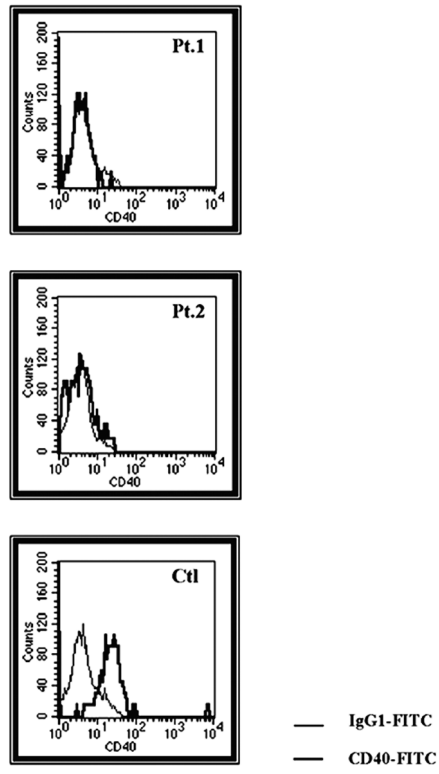

Fig. 1. CD40 is absent from the surface of B cells. Peripheral blood B cells from Pt.1 and Pt.2 and from a normal control were analyzed by flow cytometry for surface expression of CD40. PBMC were double stained for FITC anti-CD40 and PE anti-CD19 and gated on the $CD19^+$ population. Staining with mouse IgG1-FITC represented the isotype-matched internal control.

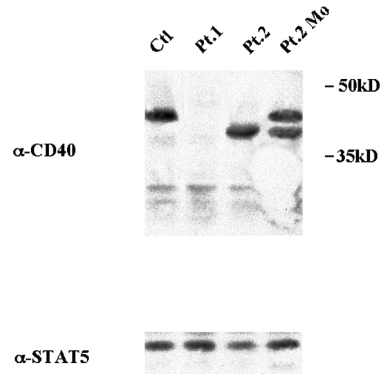

Fig. 2. Western blot analysis of CD40 expression in HIGM3 patients. Western blot experiment was performed with whole cellular extracts from B-LCLs derived from the patients and from a normal control (Ctl). Probing with an anti-CD40 polyclonal antibody, directed against the amino terminus of the protein, displays the expected 40-kDa band in the control and a lower molecular weight band in Pt.2. Both bands are present in patient's mother (Pt.2 Mo). No CD40-specific signal is detectable in Pt.1, even after prolonged exposure of the filter. (*Lower*) The same filter reblotted with an anti-STAT5 antibody as a control.

2, which correspond to the two previously described major alternative CD40 mRNA isoforms (19).

***CD40* Gene Mutations Cause HIGM3 Syndrome.** To search for the genomic mutations responsible for exon 5 skipping in the *CD40* mRNA from Pt.1, and for the absence of CD40 surface expression in Pt.2, we sequenced the respective *CD40* genomic loci. Specific primers were used to PCR amplify each exon, including flanking intronic splice sites and the branch sites. Nucleotide sequence analysis showed a single homozygous change (A455T) at the fifth base pair position in exon 5 in Pt.1 (Fig. 4), resulting in a silent mutation at codon Thr136. The mother of Pt.1 was found to be heterozygous for this substitution. Single strand conformational polymorphism analysis of exon 5 from 150 normal chromosomes ruled out the possibility that this nucleotide substitution may represent a polymorphism. Interestingly, this mutation occurs in a putative "exonic splicing enhancer", a cis-element that promotes inclusion of specific exons (20) through binding by the serine/arginine-rich splicing factors (21). Based on the observation made on other genes (i.e., SMN and BRCA1 genes), where the occurrence of nonsense, missense, or silent mutations prevent correct splicing resulting in exon skipping (20, 22–24), we speculated that skipping of exon 5 in Pt.1 may arise from disruption of a putative SF2/ASF binding motif. By applying a nucleotide frequency matrix calculation (20, 25,

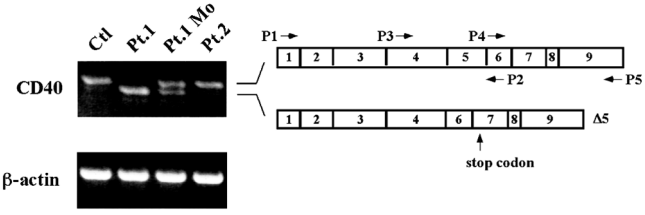

Fig. 3. RT-PCR of CD40 mRNA from PBMCs of control, Pt.1, and Pt.2, and the mother of Pt.1 (Pt.1 Mo). The normal amplification product obtained with primers P1 and P2 is 550 bp long. The lower band (Pt.1 and Pt.1 Mo) contains a deletion of 94 bp corresponding to exon 5 (Δ5 in the figure). Both amplification products were cloned and sequenced. Also indicated are the position of additional primers used in this work and the stop codon created by skipping of exon 5. (*Lower*) A control RT-PCR reaction performed with β-actin specific primers.

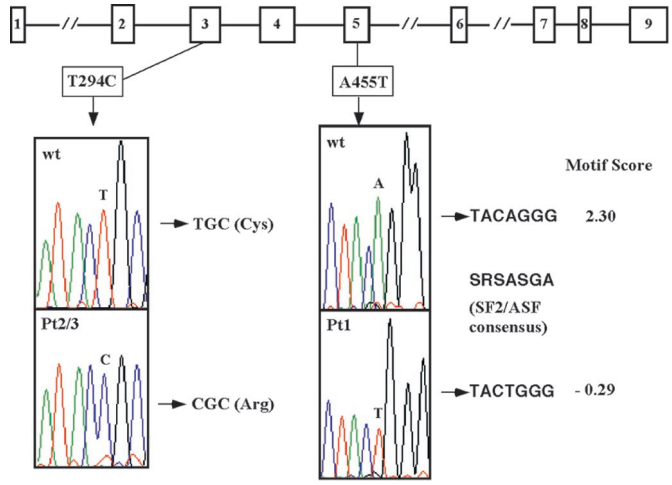

Fig. 4. Genomic organization of the *CD40* gene, showing the positions of the point mutations and the sequence data (sense strand) of the relevant regions (exon 3, nucleotides 290–296, and exon 5, nucleotides 451–458, respectively). In Pt.2 and Pt.3, the T to C substitution at nucleotide 294 changes codon 83 from Cys to Arg. In Pt.1, the A to T substitution at nucleotide 455 is a silent mutation that occurs within a putative binding motif for the SF2/ASF protein. Base pair numbers are designated according to CD40 mRNA sequence (accession no. NM 001250). Also indicated are the scores for the normal and mutant exon 5 sequences obtained after calculating the frequency matrices derived from a pool of functional enhancer sequences selected *in vitro* (25). A score above 1.956 indicates a bona fide SF2/ASF binding motif (the consensus motif is indicated: S = G or C, R = A or G).

26), we found that the A455T mutation reduces the score for the SF2/ASF motif in exon 5 from a highly significant to an essentially null value (Fig. 4).

Genomic DNA sequence analysis performed in Pt.2 and Pt.3 showed that they are both homozygous for a T294C nucleotide substitution in exon 3, resulting in a Cys to Arg substitution at residue 83. This change occurs in the extracellular cysteine-rich domain of CD40, which is highly conserved among members of the tumor necrosis factor receptor (TNFR) superfamily (27). Change of the Cys sulfidryl group to the positively charged Arg is likely to interfere with formation of intrachain disulfide bonds and protein folding, thus preventing membrane localization of CD40, and might also affect protein migration pattern in SDS/PAGE (Fig. 2). Alternatively, it is possible that the mutant protein undergoes aberrant cleavage.

The Mutation Identified in Pt.1 Causes the Exclusion of Exon 5 from mRNA. To exclude that additional inherited factors, other than the nucleotide substitution identified in the *CD40* gene of Pt.1, might be responsible for exon 5 skipping, we performed an exon trapping experiment. This method, originally developed as a rapid approach to identify and isolate exons from complex mammalian genomic DNA (17, 18), is based on the selection of 5′ and 3′ splice sites that are functional in COS-7 cells. Thus, it provides a simple way to study the splicing functionality of the mutant and wild-type *CD40* exon 5 sequences independently of the patient's genetic background. Briefly, genomic DNA containing the human *CD40* exon 5, flanked by its 5′ and 3′ splice sites, was inserted into an intron of the HIV 1 *tat* gene, contained within the pSPL3 plasmid. After transfection in COS-7 cells, mRNA transcribed from an upstream SV40 promoter was analyzed by RT-PCR for the inclusion of human *CD40* exon 5, by using primers complementary to the vector exon sequences flanking the *tat* intron. A vector/vector splicing event occurred when COS-7 cells were transfected with plasmid that did not contain subcloned genomic DNA, generating a major PCR

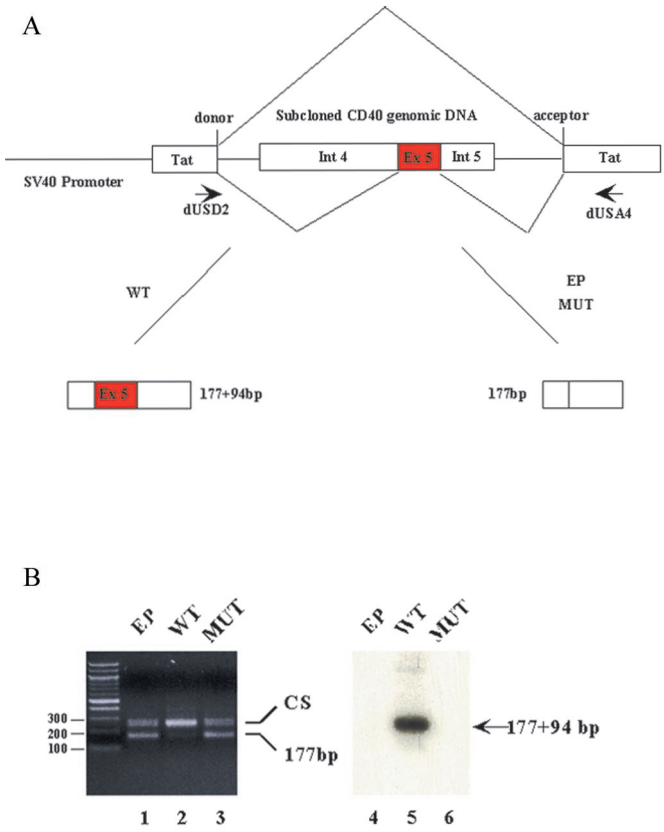

Fig. 5. Exon trapping experiment from the human *CD40* genomic clones. (*A*) Schematically shows the potential splicing events generated in the exon trapping procedure. COS-7 cells were transfected with the pSPL3 vector containing the *CD40* genomic sequence corresponding to either the wild-type (WT) or the mutated (MUT) exon 5 and the flanking introns, or with the empty plasmid (EP). RNAs from transfected COS-7 cells were isolated, converted to cDNA, and amplified (primers used in the secondary amplification reaction are indicated). The resulting PCR products were analyzed by 2% agarose gel electrophoresis (*B*), subcloned, and sequenced. The 177-bp fragment was derived from the splicing occurring between vector 5′ and 3′ splice sites (lane 1). This product was absent when the cells were transfected with the construct containing the wild-type *CD40* exon 5 sequence (lane 2), but it reappeared when the *CD40* exon 5 carried the A455T mutation present in Pt.1 (compare lane 2 and 3). The 271-bp specific fragment present in lane 2 corresponded to the product derived from the splicing occurring between the vector and the *CD40* exon 5, and it included the exon 5. A weakly stained 300-bp fragment was present in lanes 1 and 3 (CS in the figure) and corresponded to a product derived from cryptic splice sites, which are present into the intron of the HIV 1 *tat* gene. Southern blot analysis of the PCR products, performed with a probe corresponding to the *CD40* exon 5, confirmed that only the specific 271-bp fragment in lane 2 trapped the exon 5 (lane 5).

product of 177 bp (Fig. 5, lane 1), and several less abundant larger products because of cryptic splicing events (CS in Fig. 5). A specific DNA fragment of 271 bp (177 + 94 bp) was generated when splicing occurred between splice sites from the subcloned wild-type *CD40* genomic DNA and the vector, thus including exon 5 (Fig. 5, lane 2). On the other hand, when COS-7 cells were transfected with plasmid that contained the mutant *CD40* genomic construct carrying the A455T nucleotide substitution identified in Pt.1, trapping of exon 5 was not observed (Fig. 5, lane 3), and the only specific PCR product corresponded to the vector/vector splicing event described for the pSPL3 plasmid alone (compare lane 3 to lane 1 in Fig. 5). To exclude the possibility that some residual vector/exon 5/vector splicing events occurred in the presence of the A455T nucleotide substitution, we performed a Southern blot analysis by using *CD40* exon 5 as a probe. As expected, a specific signal could be seen only when the subcloned *CD40* genomic fragment corresponded to the wild-type *CD40* sequence (Fig. 5, lanes 5 and 6). These data were confirmed by cloning and sequencing the PCR fragments in lanes 1, 2, and 3; only the 271-bp fragment in lane 2 contained exon 5 of the *CD40* gene. This experiment showed that the mutation described in Pt.1 was indeed sufficient to cause skipping of exon 5.

Immunological Studies of CD40-Deficient Patients. We further investigated the consequences of lack of CD40 expression on B cell differentiation in both Pt.1 and Pt.2, compared with normal age-matched controls. Peripheral blood B cells were analyzed for IgD, IgM, and CD20 surface expression, as well as for IgD, CD27, and CD20 expression, by three-color staining. Whereas in normal age-matched controls 20–30% of peripheral B cells are isotype-switched cells, corresponding to IgM/IgD double negative cells, virtually all B cells from Pt.1 and Pt.2 coexpressed IgD and IgM. As expected, the proportion of IgD^- $CD27^+$ isotype-switched memory B cells population was greatly diminished in these patients (0.1 and 0.5% in Pt.1 and Pt.2, respectively, as compared with 12–21% in age-matched controls; data not shown). In contrast, the IgD^+ $CD27^+$ subpopulation of unswitched B cells is normally present in HIGM3 patients (5% and 10% in Pt.1 and Pt.2, respectively). Whether this subset corresponds to bona fide postgerminal center cells or represents a distinct subpopulation of B cells remains an open question.

The ability of B cells derived from Pt.1 and Pt.2 to undergo Ig isotype switching in the presence of CD40 agonists was directly assessed *in vitro* by coculturing PBMC with CDw32FcγRII-transfected L cells in the presence of anti-CD40 antibody (mAb89) and IL-10. Addition of IL-10 induced a remarkable production of IgG, IgA, and IgM in normal controls but not in the patients (Table 2).

On the whole, these data suggest that lack of CD40 expression on the surface of B cells results in defective generation of isotype-switched memory B cells and impaired class switch recombination, the same immunological profile described in patients with HIGM1 (4–7, 9, 28). Because CD40 is expressed as a trimer, it is also possible that heterozygous mutations that allow expression of CD40, but affect its function, may also result in a HIGM phenotype by exerting a dominant-negative effect. Moreover, mutations in the intracytoplasmic domain of CD40 might allow surface protein expression, preventing correct signaling and hence resulting in HIGM.

Table 2. *In vitro* immunoglobulin production in HIGM3 patients

	IgG, ng/ml			IgA, ng/ml			IgM, ng/ml		
Culture conditions	Ctl1/Ctl2	Pt. 1	Pt. 2	Ctl1/Ctl2	Pt. 1	Pt. 2	Ctl1/Ctl2	Pt. 1	Pt. 2
Resting PBMC	39/128	144	21	41/26	<2.1	<2.1	70/52	69	15
PBMC + CDw32 L cells	58/143	145	15	28/37	<2.1	<2.1	83/61	88	9
PBMC + CDw32 L cells + mAb89	41/153	109	10	34/38	<2.1	<2.1	62/54	67	12
PBMC + CDw32 L cells + mAb89 + IL10	358/323	132	15	845/706	<2.1	<2.1	1,364/2,472	88	10

Ctl1/Ctl2, two independent normal controls.

To assess the rate of somatic hypermutation in HIGM3, we analyzed the mutation frequency of the V3–23-Cμ transcripts expressed by purified $CD19^+CD27^+$ B cells from Pt.1, as previously described (29). The proportion of V3–23 somatic mutations per base pair was significantly reduced in the patient as compared with age-matched controls (0.9% vs. 2.5–6%; data not shown), indicating defective somatic hypermutation in CD40-deficient B cells.

In summary, we found that lack of CD40 surface expression causes an autosomal recessive form of hyper IgM that we propose to name HIGM3. The immunological phenotype of our patients closely resembles that of CD40-knockout mice (12, 13).

From a clinical point of view, HIGM3 is more similar to HIGM1 than to HIGM2. In fact, two of three patients suffered from severe interstitial pneumonia, and one patient had severe neutropenia. This increased susceptibility to opportunistic infections, well documented in HIGM1 but not in HIGM2 patients, who suffer mainly from recurrent bacterial infections, confirms the critical role of CD40/CD40L interaction in immune defense mechanisms toward both extracellular and intracellular pathogens (30–32).

We thank Adrian Krainer for helping us to calculate the frequency matrices for SF2/ASF motif, and Dr. Anna Villa and Dr. Annalisa Frattini. We thank the members of our laboratory and the members of the Immunopathology Laboratory at King Faisal Specialist Hospital and Research Centre for valuable discussion and support. This research was supported by Telethon (Grant E668 to L.D.N), by Ministero dell'Università e della Ricerca Scientifica e Tecnologica (cofinanziamento 99 to A.P. and Centro d'Eccellenza Innovazione Diagnostica e Tecnologica to L.D.N.), by Consiglio Nazionale delle Ricerche (biotechnology project (to L.D.N.), by Associozione Immunodeficienze Primitive, and by the European Union (Grant CT-983007 to L.D.N and A.D., and Grant QLRT-2000-01395 to L.D.N.). S.F. was supported by Telethon Fellowship 421/bi. S.F. is grateful to Cesare Rossi for love and support.

1. Banchereau, J., Bazan, F., Blanchard, D., Briere, F., Galizzi, J. P., van Kooten, C., Liu, Y. J., Rousset, F. & Saeland, S. (1994) *Annu. Rev. Immunol.* **12,** 881–922.
2. Hollenbaugh, D., Ochs, H. D., Noelle, R. J., Ledbetter, J. A. & Aruffo, A. (1994) *Immunol. Rev.* **138,** 23–37.
3. Foy, T. M., Laman, J. D., Ledbetter, J. A., Aruffo, A., Claassen, E. & Noelle, R. J. (1994) *J. Exp. Med.* **180,** 157–163.
4. Allen, R. C., Armitage, R. J., Conley, M. E., Rosenblatt, H., Jenkins, N. A., Copeland, N. G., Bedell, M. A., Edelhoff, S., Disteche, C. M., Simoneaux, D. K., *et al*. (1993) *Science* **259,** 990–992.
5. Aruffo, A., Farrington, M., Hollenbaugh, D., Li, X., Milatovich, A., Nonoyama, S., Bajorath, J., Grosmaire, L. S., Stenkamp, R., Neubauer, M., *et al*. (1993) *Cell* **72,** 291–300.
6. DiSanto, J. P., Bonnefoy, J. Y., Gauchat, J. F., Fisher, A. & de Saint Basile, G. (1993) *Nature (London)* **361,** 541–543.
7. Fuleihan, R., Ramesh, N., Loh, R., Jabara, H., Rosen, R. S., Chatila, T., Fu, S. M., Stamenkovic, I. & Geha, R. S. (1993) *Proc. Natl. Acad. Sci. USA* **90,** 2170–2173.
8. Notarangelo, L. D., Duse, M. & Ugazio, A. G. (1992) *Immunodefic. Rev.* **3,** 101–122.
9. Korthauer, U., Graf, D., Mages, H. W., Briere, F., Padayachee, M., Malcolm, S., Ugazio, A. G., Notarangelo, L. D., Levinsky, R. J. & Kroczek, R. A. (1993) *Nature (London)* **361,** 539–541.
10. Durandy, A., Schiff, C., Bonnefoy, J. Y., Forveille, M., Rousset, F., Mazzei, G., Milili, M. & Fischer, A. (1993) *Eur. J. Immunol.* **23,** 2294–2299.
11. Xu, J., Foy, T. M., Laman, J. D., Elliott, E. A., Dunn, J. J., Waldschmidt, T. J., Elsemore, J., Noelle, R. J. & Flavell, R. A. (1994) *Immunity* **1,** 423–431.
12. Kawabe, T., Naka, T., Yoshida, K., Tanaka, T., Fujiwara, H., Suematsu, S., Yoshida, N., Kishimoto, T. & Kikutani, H. (1994) *Immunity* **1,** 167–178.
13. Castigli, E., Alt, F. W., Davidson, L., Bottaro, A., Mizoguchi, E., Bhan, A. K. & Geha, R. S. (1994) *Proc. Natl. Acad. Sci. USA* **91,** 12135–12139.
14. Callard, R. E., Smith, S. H., Herbert, J., Morgan, G., Padayachee, M., Lederman, S., Chess, L., Kroczek, R. A., Fanslow, W. C. & Armitage, R. J. (1994) *J. Immunol.* **153,** 3295–3306.
15. Conley, M. E., Larche, M., Bonagura, V. R., Lawton, A. R., 3rd, Buckley, R. H., Fu, S. M., Coustan-Smith, E., Herrod, H. G. & Campana, D. (1994) *J. Clin. Invest.* **94,** 1404–1409.
16. Revy, P., Muto, T., Levy, Y., Geissmann, F., Plebani, A., Sanal, O., Catalan, N., Forveille, M., Dufourcq-Labelouse, R., Gennery, A., *et al*. (2000) *Cell* **102,** 565–575.
17. Buckler, A. J., Chang, D. E., Graw, S. L., Brook, J. D., Haber, D. A., Sharp, P. A. & Hausman, D. E. (1991) *Proc. Natl. Acad. Sci. USA* **88,** 4005–4009.
18. Church, D. M., Stotler, C. J., Rutter, J. L., Murrell, J. R., Trofatter, J. A. & Buckler, A. J. (1994) *Nat. Genet.* **6,** 98–105.
19. Tone, M., Tone, Y., Fairchild, P. J., Wykes, M. & Waldmann, H. (2001) *Proc. Natl. Acad. Sci. USA* **98,** 1751–1756.
20. Liu, H.-X., Cartegni, L., Zhang, M. Q. & Krainer, A. R. (2001) *Nat. Genet.* **27,** 55–58.
21. Valcarcel, J. & Green, M. R. (1996) *Trends Biochem. Sci.* **21,** 296–301.
22. Lorson, C. L., Hahnen, E., Androphy, E. J. & Wirth, B. (1999) *Proc. Natl. Acad. Sci. USA* **96,** 6307–6311.
23. Monani, U. R., Lorson, C. L., Parsons, D. W., Prior, T. W., Androphy, E. J., Burghes, A. H. M. & McPherson, J. D. (1999) *Hum. Mol. Genet.* **8,** 1177–1183.
24. Lorson, C. L. & Androphy, E. J. (2000) *Hum. Mol. Genet.* **9,** 259–265.
25. Liu, H.-X., Zhang, M. & Krainer, A. R. (1998) *Genes Dev.* **12,** 1998–2012.
26. Liu, H.-X., Chew, S. C., Cartegni, L., Zhang, M. Q. & Krainer, A. R. (2000) *Mol. Cell. Biol.* **20,** 1063–1071.
27. Locksley, R. M., Killeen, N. & Lenardo, M. J. (2001) *Cell* **104,** 487–501.
28. Agematsu, K., Nagumo, H., Shinozaky, K., Hokibara, S., Yasui, K., Terada, K., Kawamura, N., Toba, T., Nonoyama, S., Ochs, H. D. & Komiyama, A. (1998) *J. Clin. Invest.* **102,** 853–860.
29. Levy, Y., Gupta, N., Le Deist, F., Garcia, C., Fisher, A., Weill, J. C. & Reynaud, C. A. (1998) *Proc. Natl. Acad. Sci. USA* **95,** 13135–13141.
30. Wiley, J. A. & Harmsen, A. G. (1995) *J. Immunol.* **155,** 3525–3529.
31. Noelle, R. J. (1996) *Immunity* **4,** 415–419.
32. Stout, R. D., Suttles, J., Xu, J., Grewal, I. S. & Flavell, R. A. (1996) *J. Immunol.* **156,** 8–11.